Materials Letters 179 (2016) 12–15

Contents lists available at ScienceDirect

Materials Letters

journal homepage: www.elsevier.com/locate/matlet

Grain refinement of intermetallic compounds in the Cu–Sn system under high pressure torsion

A. Korneva [a], B. Straumal [b,c,d,*], R. Chulist [a], A. Kilmametov [c], P. Bała [e,f], G. Cios [e], N. Schell [g], P. Zięba [a]

[a] Institute of Metallurgy and Materials Science, Polish Academy of Sciences, 25 Reymonta Street, 30-059 Krakow, Poland
[b] Institute of Solid State Physics, Russian Academy of Sciences, Ac. Ossipyan str. 2, 142432 Chernogolovka, Moscow, Russia
[c] Karlsruhe Institute of Technology (KIT), Institute of Nanotechnology, Hermann-von-Helmholtz-Platz 1, 76344 Eggenstein-Leopoldshafen, Germany
[d] Laboratory of Hybrid Nanomaterials, National University of Science and Technology «MISiS», Leninskii prosp. 4, 119049 Moscow, Russia
[e] AGH University of Science and Technology, Academic Centre for Materials and Nanotechnology, 30 Mickiewicza Av., 30-059 Krakow, Poland
[f] Faculty of Metals Engineering and Industrial Computer Science, AGH University of Science and Technology, 30 Mickiewicza Av., 30-059 Krakow, Poland
[g] Institute of Materials Research, Helmholtz-Zentrum Geesthacht, Max-Planck-Strasse 1, D-21502 Geesthacht, Germany

ARTICLE INFO

Article history:
Received 20 April 2016
Received in revised form
6 May 2016
Accepted 8 May 2016
Available online 9 May 2016

Keywords:
Nano-crystalline metals
Microstructure
Thermodynamics and kinetics
Cu–Sn alloy
High-pressure torsion

ABSTRACT

The Cu–36 wt% Sn alloy was subjected to the high pressure torsion (HPT) at room temperature. Before deformation the microstructure was composed of alternating coarse-grained plates of the ζ and ε compounds (Hume-Rothery electronic phases). HPT led, as usual, to the strong grain refinement and increase of dislocation density. However, the macroscopic shape of ζ and ε plates remained unchanged. It means that the refinement took place in each phase individually, i.e. inside the respective ζ and ε plates. High angle grain boundaries are more pronounced in ε phase. This unusual behavior of the alloy is connected with a high hardness of the ζ and ε intermetallic compounds.

1. Introduction

Severe plastic deformation (SPD) usually induces a strong grain refinement and intermixing of phases. SPD frequently leads to various phase transformations, like formation [1,2] or decomposition of a supersaturated solid solutions [3–5], dissolution of phases [5–8], amorphization of crystalline phases [9–11] or formation of nanocrystals during decomposition of amorphous phase [12,13]. These phase transformations were mostly observed in alloys with fcc, bcc or hcp structures. However, the response to SPD of intermetallic phases with more complex crystal structures is rarely reported in the literature. Therefore, the copper–tin alloys, with Hume Rothery phases (or electronic compounds) having complex crystal structure was used to study the influence of SPD on microstructure and phase transformations in this system. Hume Rothery phases are known to exist when atoms with valence between two and five (like Sn, Zn, In) are added to a matrix composed of single valence atoms (Cu, Ag or Au) [14,15]. Usually, they appear in a certain sequence according to the increasing electron concentration. The aim of this work is to investigate the high pressure torsion (HPT) of Cu–36 wt% Sn alloy, where various Hume-Rothery phases (α, γ, δ, ε or ζ) exist at different temperatures.

2. Experimental

The Cu–36 wt% Sn alloy was manufactured by inductive melting in vacuum from high purity 5 N copper and tin. The ø10 mm ingots were cut by spark erosion into 0.7 mm thick discs. They were subjected to HPT in a Bridgman anvil chamber (W. Klement GmbH, Lang, Austria) at 7 GPa, five revolutions, 1 rpm. The samples for structural investigations were cut at a distance of 3 mm from the center of a deformed disc. For the metallographic investigations the samples were ground with SiC grinding paper and polished with 6, 3 and 1 μm diamond pastes. The scanning electron microscopy (SEM) was carried out on a Philips XL30 microscope equipped with a LINK ISIS energy-dispersive X-ray spectrometer (EDS) produced by Oxford Instruments. The electron backscattering diffraction (EBSD) was carried out using the FEI Quanta 3D FEGSEM instrument. The resolution of EBSD maps was

* Corresponding author at: Institute of Solid State Physics, Russian Academy of Sciences, Ac. Ossipyan str. 2, 142432 Chernogolovka, Moscow, Russia.
E-mail address: straumal@issp.ac.ru (B. Straumal).

http://dx.doi.org/10.1016/j.matlet.2016.05.059
0167-577X/

80 nm. The transmission electron microscopy (TEM) was performed by TECNAI G2 FEG super TWIN (200 kV) microscope equipped by energy dispersive X-ray (EDX) spectrometer manufactured by EDAX. TEM foils were prepared by the focused ion beam (FIB) technique. Phase analysis was made by synchrotron irradiation and a 2D detector using P07B line in DESY, Hamburg, Germany. The wave length was 1.4235 nm (87.1 KeV). The use of such an energy allowed experiments in transmission mode resulting in much better grain statistic compared to the conventional X-ray diffraction. To index the Kikuchi pattern and synchrotron diffractions, the following crystal structures were used: the hexagonal ζ phase ($Cu_{10}Sn_3$) with $P6_3$ space group and $a=0.7330$ nm, $c=0.7864$ nm lattice parameters, the orthorhombic ε phase (Cu_3Sn) with the *Cmcm* space group and $a=0.5529$ nm, $b=4.7756$ nm, $c=0.4323$ nm, the cubic ($Cu_{41}Sn_{11}$) with *F*43 m space group and $a=1.7980$ nm [16]. The hardness measurements were performed using an AGILENT G200 nanoindenter with XP head with an indentation load of 100 mN.

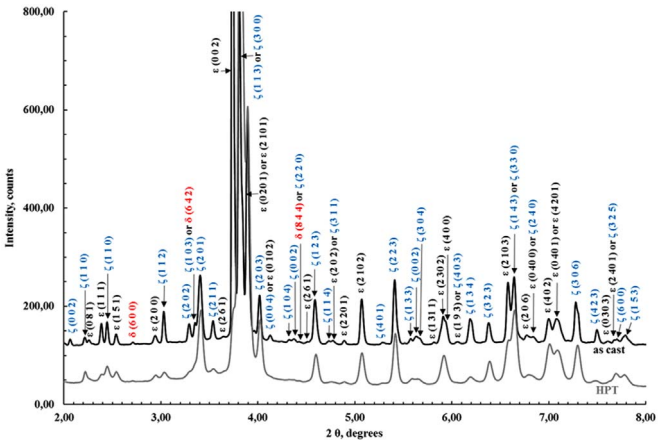

Fig. 2. Synchrotron X-ray diffraction pattern of the Cu–36 wt% Sn alloy: as-cast (top curve) and after HPT (bottom curve).

3. Results and discussion

The as-cast Cu–36 wt% Sn alloy consists of alternating plates with thickness of about 100 μm (appearing dark and bright in Fig. 1a). According to the EDS analysis, the "dark" phase could be either ζ or δ, and bright one should be ε. However, the X-ray analysis (Fig. 2) excludes the existence of δ phase confirming only the ζ and ε phases. A detailed study of the as-cast microstructure by BSE and EBSD (Fig. 1) reveals that parallel ζ plates have the same orientation and are almost single-crystalline. The ε phase is also composed of parallel plates with same orientation. However, within these plates some minor grains and subgrains can be detected (Fig. 1d). In some locations these small grains spread out across the whole ε plate (Fig. 1a).

The SEM micrographs of samples after HPT are shown in Fig. 1b. The shape of ζ and ε plates is almost unaffected by the strong deformation. The ζ plates and ε were not broken and their thickness has not changed (Fig. 1b). Moreover, the interface between two phases remained clearly visible. Only a high amount of cracks across the ε plates were observed. Nevertheless, the very poor Kikuchi patterns obtained after HPT reveal the high

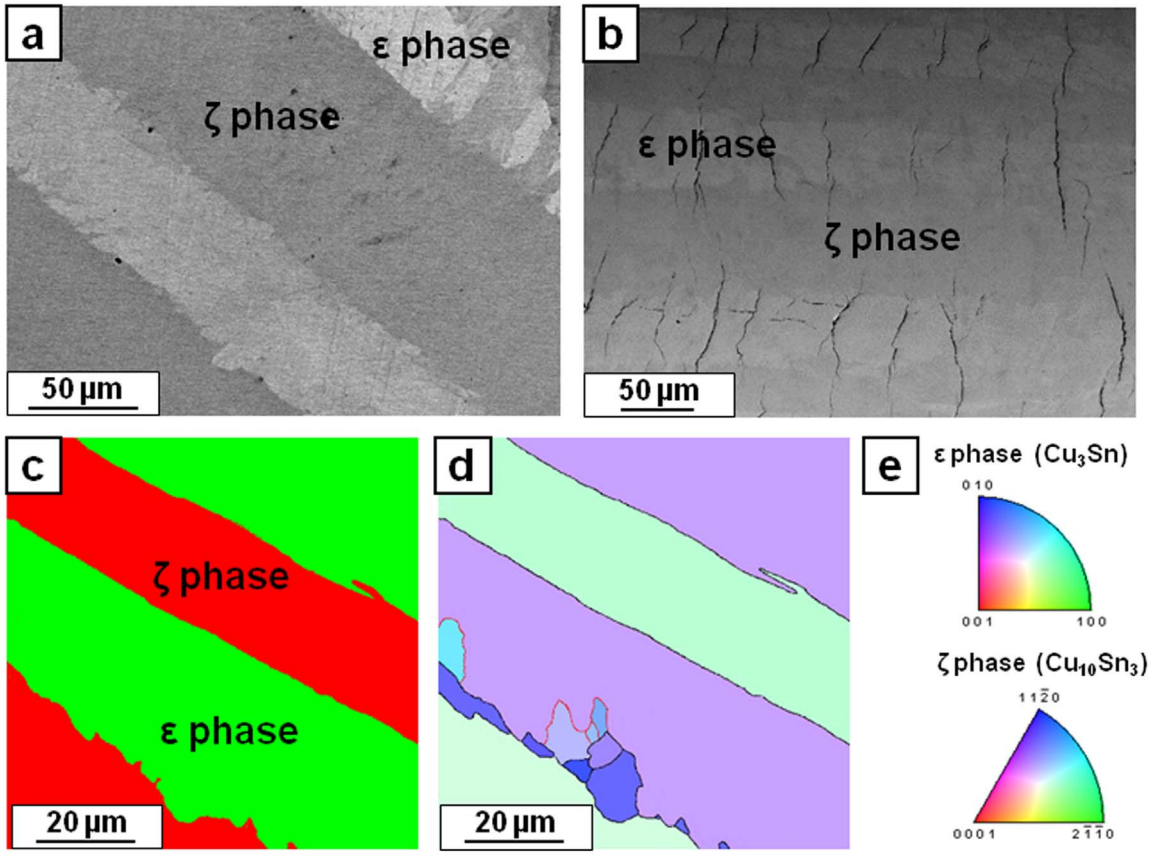

Fig. 1. SEM micrographs in BSE mode of the Cu–36 wt% Sn alloy (a) as-cast and (b) after HPT. SEM/EBSD phase map (c) and orientation map (d) of the as-cast Cu–36 wt% Sn alloy with standard unit triangles for orthorhombic ε and hexagonal ζ phases (e). Low angle grain boundaries with the misorientation angle between 3 and 15° and high angle grain boundaries with the misorientation angle between 15 and 65° are marked by red and black lines, respectively (d).(For interpretation of the references to color in this figure legend, the reader is referred to the web version of this article.)

Table 1
Sn concentration in the phases, wt%, EDS/SEM.

Phase	As cast	As cast + HPT	Reference data [18]
Phase appearing dark in Fig. 1	32.7 ± 0.6	33.0 ± 0.7	ζ (32.2–35.2) δ (31.8–33.2)
Phase appearing bright in Fig. 1	37.4 ± 0.7	37.3 ± 0.7	ε (37.7–39.5)

dislocation density after HPT.

The chemical composition of ζ and ε plates after HPT did not change in comparison to the initial ones (Table 1). Thus, no mass transfer during to SPD was observed. In the letter [17] where the ε phase and δ phase ($Cu_{41}Sn_{11}$) were observed after HPT using conventional X-ray diffraction (XRD). Based on this data the incorrect statement about decomposition of the ζ phase into the mixture of the δ and ε phases was made due to the complex structure of all three phases [17]. As most of the peaks coming from δ, ζ and ε phases are very close to each other or even overlap (Fig. 2), the conventional XRD provides a very questionable data especially if dealing with a strongly deformed and textured material. Therefore, in order to determinate the existence of these three phases accurately, the synchrotron diffraction analysis was performed in this work. Fig. 2 depicts integrated X-ray diffraction patterns of the Cu–36 wt% Sn alloy before and after HPT taken on a 2D detector with a high resolution (3450 × 3450). These diffraction patterns confirm dominating presence of the ε and ζ phase before and after HPT. A very small amount of the δ phase can be seen as well (the reflection (600) in Fig. 2). However, the same small reflection from the δ phase can be also detected after HPT. This additionally supports the fact that during HPT no significant phase transformation occurs. Further examination of the X-ray synchrotron diffraction data reveals continuous diffraction rings and a characteristic broadening. A diffraction line can broaden both due to lattice defects (dislocations) and very low grain size. In order to study the microstructure at the nanoscale, the TEM observations were performed.

The thin foil was cut by FIB technique along the line perpendicular to the interface between ζ and ε plates in order to obtain both phases in one foil. The TEM micrographs of deformed material are shown in Fig. 3. The ζ phase was characterized by a high dislocation density without well-defined grain boundaries inside a ζ plate while the ε phase forms the lamellar grains with a 50–400 nm width (Fig. 3a, b). The selected area electron diffractions (SAED) separately taken from these regions (bottom corner in Fig. 3a, b) clearly confirmed the both phases. The electron diffraction obtained from an area of about 55 μm^2 showed discontinuous rings and some elongated spots (upper corner in Fig. 3a, b). The discontinuous rings are likely associated with the existence of high-angle boundaries while the elongated spots are attributed to the low-angle grain boundaries. The high-angle boundaries are more clearly defined in the ε phase (Fig. 3b).

In order to understand why the primary plates of the ζ and ε phases maintained their shape during HPT, the microhardness was measured. The hardness of the ζ and ε intermetallic phases before HPT reached 5.4 ± 0.1 and 4.6 ± 0.3 GPa, respectively. These values are relatively high especially if compared to the soft Cu matrix in a Cu–14 wt% Sn alloy after annealing at 320 °C (1.8 ± 0.2 GPa) [18]. After HPT, the hardness of both phases reached a value of 5.7 ± 0.6 GPa. Thus, the hardness of the ζ phase increased slightly, only by 6% due to increase of dislocations density, while the hardness of the ε phase increased notably by 23% due to grain refinement, increase of dislocations density and internal stresses. It seems that the primary plates of the ζ and ε phases neither broke nor changed their thickness after deformation because of

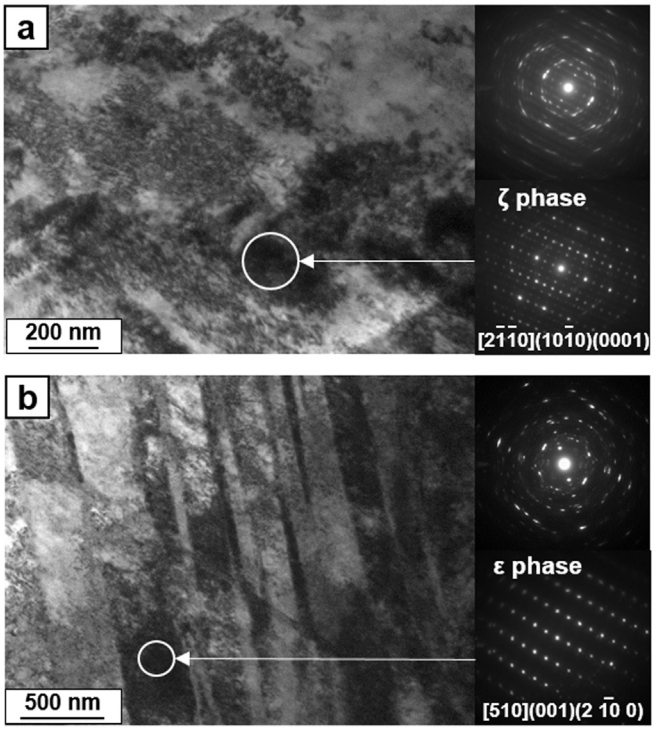

Fig. 3. TEM micrographs of ζ (a) and ε (b) plates of the Cu–23 at% Sn alloy after HPT with SAED patterns. SAED patterns obtained from the whole visible area in Figs. (a) and (b) are placed in the upper right corner of these Figs. SAED patterns obtained from the separated ζ and ε grains (marked by rings) are placed in the bottom right corner in Figs. (a) and (b).

their high hardness. The Cu–22 wt% In alloy [20], before HPT contained hard precipitates of intermetallic δ phase (2 GPa) in the soft Cu-matrix (1 GPa). After HPT the strong grain refinement of the Cu-matrix took place, while the hard δ phase appeared unaffected, i.e. neither broke nor refined. As a result of HPT, the hardness of the α phase increased by about 90%, while the hardness of intermetallic δ phase increased by only 38%. This unusual behavior of the δ phase was related to its high hardness. Similar situation was observed also in the Cu-14 wt% Sn alloy subjected to HPT [19]. It was recently shown [21,22] that the deformation-induced structure transformations are determined by the cumulative abilities of individual crystalline phases in the alloy. It was also concluded that the mechanical factor (Young's modulus) determines the ability of crystalline alloys and individual crystalline phases to deformation-induced transformation upon high-pressure torsion.

4. Conclusions

Cu–36 wt% Sn alloy was subjected to HPT at room temperature. The microstructure of the alloy, before HPT, contained alternating (coarse-grained or even single-crystalline) plates of the ζ and ε Hume-Rothery phases. After HPT the grain refinement took place inside the ζ and ε plates. However, the shape of alternating plates remained almost unchanged. The HPT also increased dislocation density in both phases, created cracks across the ε phase plates and increased hardness of the ε phase. However, neither dissolution of phases, nor phase transformations were observed. Most likely that unusual behavior of this alloy is connected with high hardness of the intermetallic ζ and ε phases.

Acknowledgements

The structural investigations were performed according to European standard PN-ISO/IEC 17025:2005 as well as the EA-2/15 within the Accredited Testing Laboratories with the certificate No. AB 120 issued by the Polish Centre of Accreditation. The work was supported by the National Science Centre of Poland (Grant OPUS 2014/13/B/ST8/04247), the Russian Federal Ministry for Education and Science under Increased Competitiveness Program of NUST«-MISiS», by the Deutsche Forschungsgemeinschaft and Russian Foundation for Basic Research (Grant 16-53-12007).

References

[1] W. Lojkowski, M. Djahanbakhsh, G. Burkle, et al., Mater. Sci. Eng. A 303 (2001) 197–208.
[2] V.V. Stolyarov, R. Lapovok, I.G. Brodova, et al., Mater. Sci. Eng. A 357 (2003) 159–167.
[3] B.B. Straumal, B. Baretzky, A.A. Mazilkin, et al., Acta Mater. 52 (2004) 4469–4478.
[4] A.A. Mazilkin, B.B. Straumal, E. Rabkin, et al., Acta Mater. 54 (2006) 3933–3939.
[5] B. Straumal, A. Korneva, P. Zięba, Arch. Civ. Mech. Eng. 14 (2014) 242–249.
[6] Y. Ivanisenko, I. MacLaren, X. Sauvage, et al., Acta Mater. 54 (2006) 1659–1669.
[7] S. Ohsaki, S. Kato, N. Tsuji, et al., Acta Mater. 55 (2007) 2885–2895.
[8] B.B. Straumal, S.V. Dobatkin, A.O. Rodin, et al., Adv. Eng. Mater. 13 (2011) 463–469.
[9] A.A. Mazilkin, G.E. Abrosimova, S.G. Protasova, et al., J. Mater. Sci. 46 (2011) 4336–4342.
[10] V.V. Stolyarov, D.V. Gunderov, A.G. Popov, et al., J. Alloy. Compd. 281 (1998) 69–71.
[11] B.B. Straumal, A.A. Mazilkin, S.G. Protasova, et al., Kov. Mater.: Metall. Mater. 49 (2011) 17–22.
[12] A.M. Glezer, M.R. Plotnikova, A.V. Shalimova, et al., Bull. Russ. Acad. Sci. Phys. 73 (2009) 1233–1239.
[13] G.E. Abrosimova, A.S. Aronin, S.V. Dobatkin, et al., J. Metastab. Nanocryst. Mater. 24 (2005) 69–72.
[14] T.B. Massalski, U. Mizutani, Prog. Mater. Sci. 22 (1978) 151–262.
[15] Ya.S. Umanskii, Yu.A. Skakov, Physics of Metals (Atomic Structure of Metals and Alloys), Metallurgiya, Moscow, 1978 (in Russian).
[16] P. Villars, L.D. Calvert, Pearson's Handbook of Crystallographic Data for Intermetallic Phases, second ed., ASM International, USA 1991, pp. 3006–3008.
[17] B.B. Straumal, A.R. Kilmametov, Yu.O. Kucheev, JETP Lett. 100 (2014) 376–379.
[18] N. Saunders, A.P. Miodownik, Cu-Sn (Copper-Tin), in: B. Massalski (Ed.), second ed.,Binary Alloy Phase Diagrams, 2, ASM International, USA, 1990, pp. 1481–1483.
[19] A. Korneva, , B. Straumal, A. Kilmametov, Mater. Charact. (2016) (in press).
[20] A. Korneva, B. Straumal, O. Kogtenkova, et al., IOP Conf. Ser. Mater. Sci. Eng. 63 (2014) 012093.
[21] R.V. Sundeev, A.M. Glezer, A.V. Shalimova, Mater. Lett. 133 (2014) 32–34.
[22] R.V. Sundeev, A.M. Glezer, A.V. Shalimova, J. Alloy. Compd. 611 (2014) 292–296.